Journal of Engineering and Applied Sciences 13 (Special Issue 13): 10735-10741, 2018
ISSN: 1816-949X

Optimized Biosensor Based on Self-Mixing Interferometer

Firas S. Mohammed and Zainab Salman Abd Al-Ameer
Department of Physics, College of Sciences, Al-Mustansiriyah University, Baghdad, Iraq

Abstract: The fields of biological and medical physics have a particularly strong correlation with biomedical sensing applications. Our research aims to contribute into the optics of biomedical measurement using the self-mixing interferometry configuration through design and simulate SMI sensing system and more parameters have to be optimized. The performance was numerically investigated for the cases of changing important system parameters such as, external cavity length, external reflectivity and concentration of the target material. The next step in the optimized technique is its implementation in bio-sensing field. For the modified configuration, one can expect to have a strong correlation between the amplitude of the main peaks appearance and the glucose concentration. The time-delay of the system is correctly identified even in the presence of the reference light which enables us to extract the chaotic signature (glucose concentration) successfully. The numerical results find that the system can be used successfully as a biosensor.

Key words: Biomedical sensing, self-mixing interferometry, glucose concentration, external cavity, parameters, biosensor

INTRODUCTION

The behavior of the Laser Diodes (LD) gave rise to some of the early studies that can be related to applications in the presence of external perturbations. For example, the technique of optical feedback interferometry, also, known as Self-Mixing Interferometry (SMI) (Donati, 2012). The main part of SMI consists of a laser and a target and the self-mixing signal is the result of the interference of the field within the laser cavity with the field back-scattered by a remote target (Vidakis and Santiago, 2015). For clarity, a self-mixing interferometer is a measurement device which is used to measure some physical phenomenon. Many factors affect the SMI signal that is obtained such as the reflectivity of the target, its distance to the laser, the ambient temperature and refractive index of the medium or any small vibrations that the set-up could undergo. The main advantages of SMI are the simple set-up, cost-effectiveness no need of an external photo-detector as the self-mixing signal is captured from a built-in photodiode within the laser diode package, the compactness and self-aligned and diffusive targets are in the capabilities of SMI (Kane and Shore, 2005). As well, the propagation direction of light that is reflected back toward input port is affected by optical circulation to reflection output light (Nazerian *et al*., 2016). For the bio-sensing, the reflected signal induced a "peak" or a "valley" considered as a possible estimation of the time delay (VanWiggeren and Roy, 1999). These pulses bear all the information on the object (target), thus, the time-delay between the pulses gives the information on the amplitude and velocity of waves (Sarimov and Muhtarov, 2016). This study aims to contribute into the optics of biomedical measurement using the self-mixing interferometry configuration. This goal will achieved through design and simulate SMI sensing system and more parameters have to be optimized. In order to obtain more stable external configurations. Moreover, investigating the biomedical-abilities of the optimized SMI bio-sensor.

MATERIALS AND METHODS

Sensing model and simulation: The SMI sensing system can be describe by solving Lang and Kobayashi (LK) equations (Acket *et al*., 1984; Shrestha, 2010) of laser diodes with optical feedback. The theoretical rate equation models consider the time dependence of the amplitude of the electric field and the dynamical interplay between the electric charge carriers and photons in the semiconductor laser cavity. The diode mirror facets, M_1 and M_2 are positioned at z = 0 and z = L with an amplitude reflection coefficient, $r_{1,}$ r_{2s} of laser facet, respectively. The external target is positioned at $z = L+L_{ext}$ with an external amplitude reflection coefficient, r_{2ext}. Where, τ_{ext} denoted the round trip delay through the external cavity of length L_{ext} and expressed as:

$$\tau_L = \tau_{ext} = \frac{2L_{ext}}{c} \quad (1)$$

Corresponding Author: Firas S. Mohammed, Department of Physics, College of Sciences, Al-Mustansiriyah University, Baghdad, Iraq

To achieve successful operation of the laser, both the phase and amplitude conditions must be fulfilled, thus:

$$|r_c| = r_2(1+k_{ext}\cos 2\pi v_c \tau_{ext}) \quad (2)$$

where, k_{ext} measuring the coupling strength (coefficient) between the two cavities and v_c is the optical frequency (Wei, 2011):

$$k_{ext} = \frac{r_{2ext}}{r_2}\left(1-|r_2|^2\right) \quad (3)$$

Similarly:

$$\varnothing_r = k_{ext}\sin\left(2\pi v_c \tau_{ext}\right) \quad (4)$$

Since, $\varnothing_r$ the round trip phase withen the compound laser cavity must meet the phase condition for lasing that is:

$$2\beta L+\varnothing_r = 2m\pi \quad (5)$$

where, β is the phase constant of the optical wave denoted as:

$$\beta = \frac{4\pi v_c \mu_e}{c} \quad (6)$$

Where:

v = The optical frequency
μ_e = The effective refractive index
c = The speed of light in vacuum

Moreover, by substituting β:

$$\frac{4\pi v_c \mu_e}{c}+\varnothing_r = 2m\pi \quad (7)$$

Finally, the phase of light with external feedback:

$$\varnothing_L = 2\pi v_c \tau_{ext} \quad (8)$$

Based on these behaviors, feedback level can be characterized by another (feedback Coefficient C) (Acket *et al*., 1984) defined as:

$$C = \frac{\tau_{ext}}{\tau_{in}} k\sqrt{1+a^2} \quad (9)$$

where, τ_{in} internal cavity round-trip time and α is the line-width enhancement factor associated with the gain changes due to carrier depletion (Nazerian *et al*., 2016). In addition, C describes how effective optical feedback is in changing the intrinsic behavior of the laser. Therefore, laser rate equations become:

$$\frac{d}{dt}E_\circ(t) = \frac{1}{2}\left[G_N N(t)-N_\circ-\frac{1}{\tau_P}\right]E_0(t) \quad (10)$$

$$\frac{d}{dt}\varnothing(t) = \frac{1}{2}\alpha G_N\left[N(t)-N_T\right] \quad (11)$$

The SMI system is based on the modulation in both the amplitude and frequency of the Semiconductor Laser (SL) output power. The modulated power is known as the SMI signal which can be used for measuring the quantities of the external target and the parameters associated with the SL itself (Yu *et al*., 1999; Donati *et al*., 1995). Let us again consider the laser diode is modeled by Mirrors M1 and M2. A fraction of the optical beam from the laser diode is backscattered into the laser diode cavity by the external target. The photodiode at the rear facet of the laser diode monitors the Power, P of the laser diode by means of photo-generated current, I = σP where, σ = spectral responsively. According to the Lang and Kobayashi's equations, the dynamics of a laser diode in the presence of feedback can be written as:

$$\frac{d}{dt}E_0(t) = \frac{1}{2}G_N\left[N(t)-N_\circ-\frac{1}{\tau P}\right]E_0(t)+ \frac{k}{\tau_L}E_0(t-\tau)\cos[\omega_0\tau+\varnothing(t)-\varnothing(t-\tau)] \quad (12)$$

$$\frac{d}{dt}\varnothing(t) = \frac{1}{2}\alpha G_N\left[N(t)-N_{Th}\right]- \frac{k}{\tau L}-\frac{E_0(t-\tau)}{E_0(t)}\sin\left[\omega_0\tau+\varnothing(t)-\varnothing(t-\tau)\right] \quad (13)$$

$$\frac{d}{dt}N(t) = R_P-\frac{N(t)}{\tau_s}-G_N\left[N(t)-N_0\right]E_0^2(t) \quad (14)$$

Where:

E(t)	=	Laser Electric field, expressed as $E(t) = E_0(t)\exp[j\omega_0\tau+\varnothing(t)]$ with normalized $E_0(t)$
$P = E_0^2(t)$	=	The optical density in the laser cavity
G_N	=	Modal Gain coefficient
N(t)	=	Average carrier (electron-hole pairs) density in the active layer
N_0	=	Carrier density at transparency
N_{th}	=	Threshold carrier density for the unperturbed laser
τ_P	=	Photon lifetime
τ_L	=	Diode cavity round trip time
τ_c	=	Carrier lifetime
R_P	=	Electric pumping term which is given by $R_P = jn/ed$
J	=	Injected current density
n	=	Conversion efficiency
e	=	Electron charge
d	=	Active layer thickness

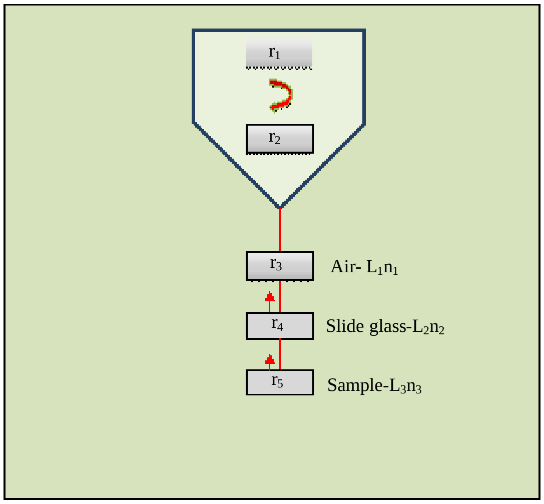

Fig. 1: Self-mixing interferometric technique for bio-sensing

Implementation of SMI system in bio-sensing: Self-mixing interferometric technique for bio-sensing is based on detect the variation in sample's refractive index. The proposed set-up is based on a multi-external cavity model, as illustrates in Fig. 1. The model includes three external cavities which consist of air, glass (slide or vessel) and sample (bio-material) for this experiment. The round-trip delay of each external cavity can be calculated as the time delay for air cavity is:

$$\tau_1 = 2\frac{L_1 n_{Air}}{c} \quad (15)$$

The time delay for air and glass cavity is:

$$\tau_2 = 2\frac{[L_1 n_{Air} + L_2 n_{Glass}]}{c} \quad (16)$$

The time delay for air, glass and sample cavity is:

$$\tau_3 = 2\frac{[L_1 n_{Air} + L_2 n_{Glass} + L_3 n_{Sample}]}{c} \quad (17)$$

Where:
- L = Internal cavity length
- L_1 = Air cavity length
- L_2 = Glass cavity length
- L_3 = Sample cavity length
- n_1 = Air refractive index
- n_2 = Glass refractive index
- n_3 = Sample refractive index

Similarly, the feedback coupling strength (coefficient) become as the feedback coupling coefficient for external air cavity k_1 as in Eq. 3. Also, the feedback coupling coefficient for air and glass cavity is:

$$k_2 = \frac{r_4}{r_2}\left(1-r_3^2\right)\left(1-r_2^2\right) \quad (18)$$

The feedback coupling coefficient for air, glass and sample cavity is:

$$k_3 = \frac{r_5}{r_2}\left(1-r_4^2\right)\left(1-r_3^2\right)\left(1-r_2^2\right) \quad (19)$$

Where:
- r_1, r_2 = The reflectivities of laser facet
- r_3, r_4, r_5 = The external reflectivities (for air, glass and sample)

RESULTS AND DISCUSSION

In this study, the mechanism of generating an SMI signal for bio-sensing application was tested by simulation the proposed sensing scheme set-up and describes the stability of dynamical behavior. The new set-up based on number of external optical components as it is shown in Fig. 1. The performance will be numerically investigated in more details for the cases of a change of important system parameters such as (external cavity length, external reflectivity, refractive index for target). All the involved parameters of the semiconductor laser and their values used in our numerical model are listed in Table 1 (Vidakis and Santiago, 2015; Fan *et al*., 2015).

Effect of external cavity length: In this study, the values of the reflectivities (r_3 and r_4) are fixed at (0.04) and (0.02) respectively. While the refractive indexes for the air (n_1) and slide glass (n_2) are fixed at (1.00271) and (1.5175), respectively (Vidakis and Santiago, 2015). Moreover, the cavity lengths L_1 and L_2 varied from (60-70 mm) for the first one and from (1-1.3 mm) for the other, in order to improve the chaotic behavior. The characteristics of the electric field, phase of electric field, carrier density, output power and phase attractor, for the generated signal of semiconductor laser under the effect of external cavity (without target) are shown in Fig. 2 and 3.

The effect of increasing the air cavity length was demonstrated in Fig. 2 while the effect of increasing the glass slide cavity length (round trip time) was studied and demonstrated in Fig. 3, The best performance results are obtained at L_2 = 1.1 and L_1 = 66 mm as shown in Fig. 3b. For the bio-sensing part, there is possibility for modifying the system simulation with two feedbacks. The power spectrum of the stable periodic light (reference) is modulated by the target feedback signal (chaotic signature). Once the setups of the two external cavities are calibrated, the target signatures can be identified with our technique. The target was chosen as a blood-glucose

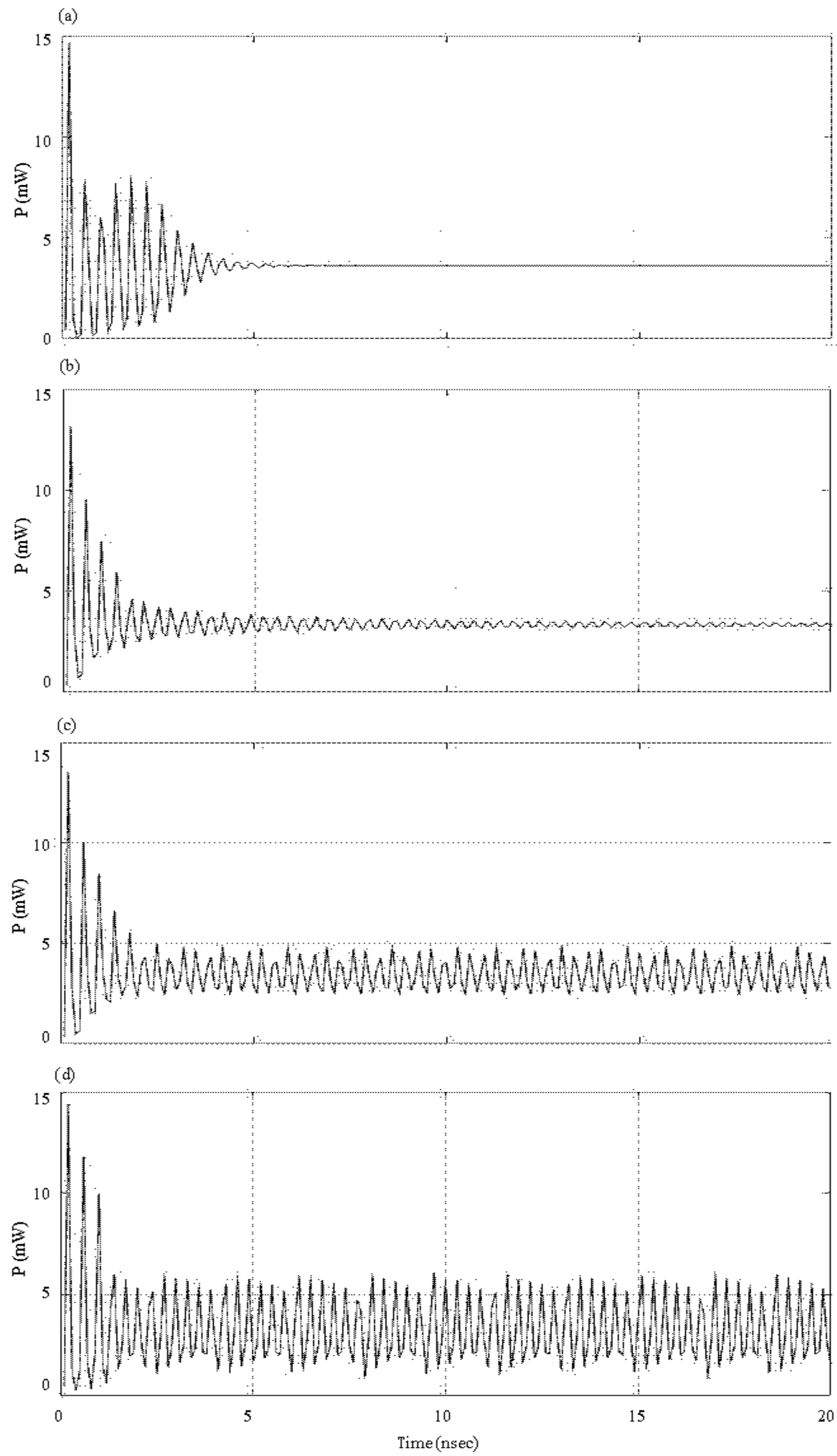

Fig. 2: Characterizations of the output power when: a) $L_1 = 60$; b) $L_1 = 62$; c) $L_1 = 64$; d) $L_1 = 68$ mm and $L_2 = 1$ mm

solutions which forms an external cavity with length (L_3 = 3 mm), refractive index (n_3) and reflectivity (r_5 = 0.20), respectively. This led to set-up where the reflective solution and the set-up cavity were separated.

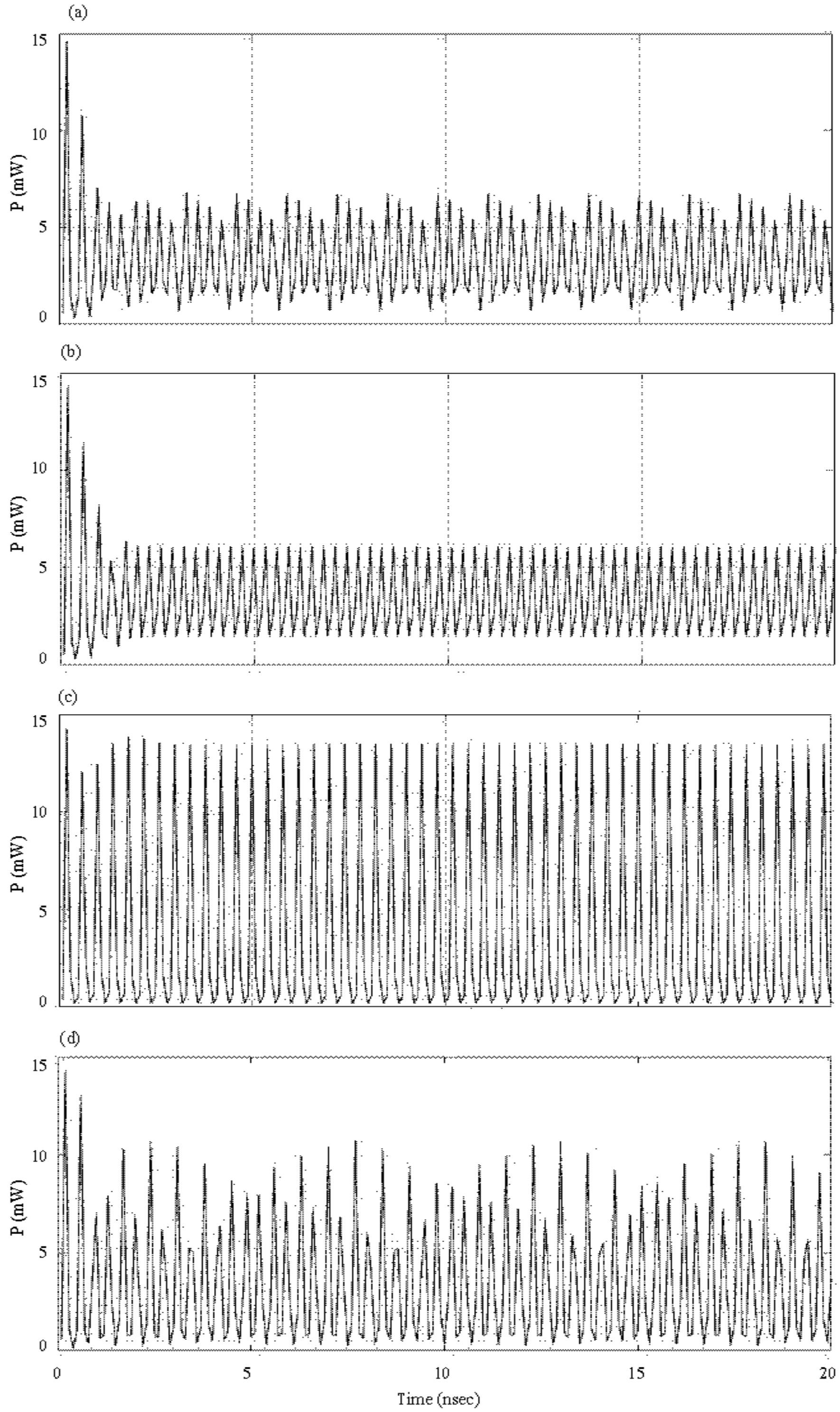

Fig. 3: Characterizations of the output power when: a) $L_2 = 1$; b) $L_2 = 1.1$; c) $L_2 = 1.2$; d) $L_2 = 1.3$ mm and $L_1 = 66$ mm

The refractive index of the solutions slightly changed when the glucose concentration (gc) is changing gradually as it seen in Fig. 4 (Yeh, 2008).

Table 2 demonstrates fasting blood glucose concentrations for people with and without diabetes.

It was shown in Fig. 5, the separation in the delay time and chaotic intensity in time series of the chaotic and stable signals in the proposed system. As a result, the amplitude of the reference light small and stable, thus, the quality of the recovered chaotic signature can be quite clear and the information extraction becomes easier. However, the chaotic signals may not provide enough information with quite large reference amplitude, agree with Zhou and Lai (1999). Therefore, these results are agreeable with the results by Audrey *et al.* (2018) which works revealed the variation of output signals associated with target concentrations and optical path lengths.

Table 1: Parameters values of semiconductor laser used in the simulation

Parameters	Values
λ	787 (nm)
α	3.7
I_{th}	20.5 (mA)
I_t	1.3 (7)*I_{th}
G_N	$8.4*10^{-13}$ (m^3 sec^{-1})
N_{th}	$2.018*10^{24}$ (m^{-3})
N	$1.4*10^{24}$ (m^{-3})
L	100 (μm)
μ_e	4
μ	3.4
V	$1.2*10^{-16}$ (m^3)
τ_p	2 ps
τ_c	2 ns
τ_{in}	8 ps
$r_{1,2}$	0.95

Where λ is the wavelength, I_{th} is threshold current, I_t injection current, μ effective mode index and V active region volume. The SMI sensing system can be described by re-written and solving equations (3.20, 3.21 and 3.22) after substitute the time delay and feedback coupling strength coefficients as written in equations (3.24 and 3.26)

Table 2: Blood sugar levels

Variables (mg/dL)	Min. (gc)	Max. (gc)
Normal	70	99
Pre-diabetes	100	125
Diabetes	126	200

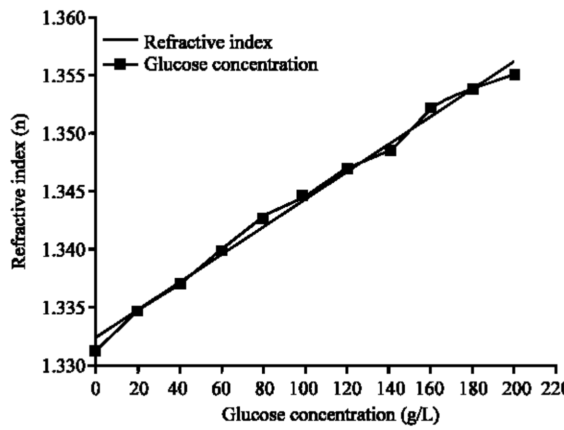

Fig. 4: The variation of average refractive index with glucose concentration

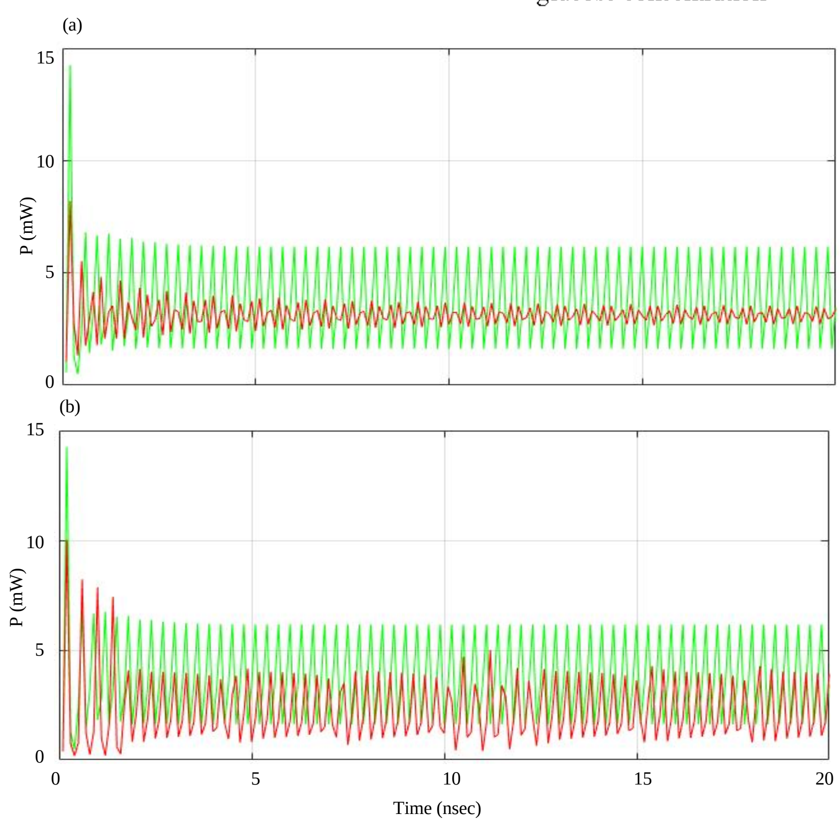

Fig. 5: Continue

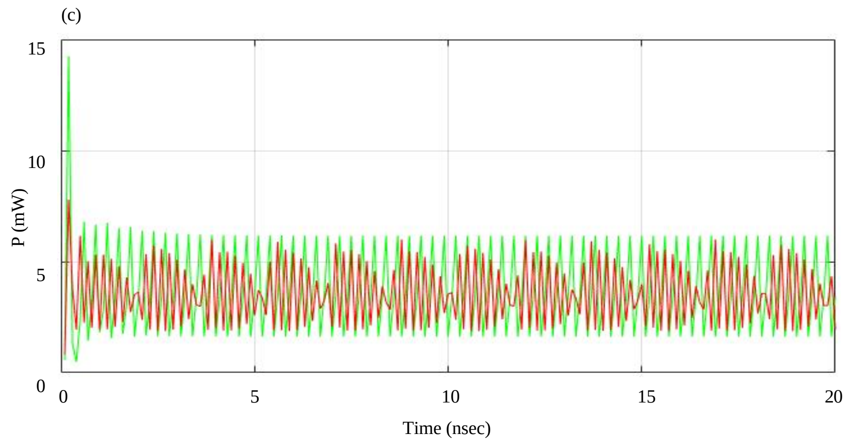

Fig. 5: Characterizations of the output power: a) n_3 = 1.342, gc = 70; b) n_3 = 1.347, gc = 120; c) n_3 = 1.349, gc = 140 and r_3 = 0.20

CONCLUSION

In this study, the overall scheme is extremely complicated and more parameters have to be simultaneously optimized. Improvements of the system are achieved by adjusting the slide cavity. For the modified configuration, one can expect to have a strong correlation between the amplitude of the main peaks appearance and the glucose concentration. Furthermore, the time-delay of the system is correctly identified even in the presence of the reference light which enables us to extract the chaotic signature (glucose concentration) successfully. The numerical results find that the implemented system can be used successfully as a biosensor.

REFERENCES

Acket, G., D. Lenstra, A. Den Boef and B. Verbeek, 1984. The influence of feedback intensity on longitudinal mode properties and optical noise in index-guided semiconductor lasers. IEEE. J. Quantum Electron., 20: 1163-1169.

Audrey, K.C., P.E. Huong, T.V.H. Ong and T.I.N. Xavier, 2018. A handheld technology for optical monitoring of transcutaneous blood oxygen saturation. Intl. J. Eng. Technol., 7: 122-126.

Donati, S., 2012. Developing self-mixing interferometry for instrumentation and measurements. Laser Photonics Rev., 6: 393-417.

Donati, S., G. Giuliani and S. Merlo, 1995. Laser diode feedback interferometer for measurement of displacements without ambiguity. IEEE. J. Quantum Electron., 31: 113-119.

Fan, Y., B. Liu, Y. Yu, J. Xi and Q. Guo *et al*., 2015. Analysis on the transient of a self-mixing interferometry sensing system. Proceedings of the 2015 IEEE Region 10th International Conference on TENCON, November 1-4, 2015, IEEE, Macao, China, ISBN:978-1-4799-8639-2, pp: 1-3.

Kane, D.M. and K.A. Shore, 2005. Unlocking Dynamical Diversity: Optical Feedback Effects on Semiconductor Lasers. Wiley Publishing Company, Hoboken, New Jersey, USA., Pages: 339.

Nazerian, V., T.N. Alireza and E.P.A. Iman, 2016. Switching characteristics of SOA-assisted all-optical sagnac interferometer switch for picosecond pulses. J. Eng. Appl. Sci., 11: 751-759.

Sarimov, L. and N. Muhtarov, 2016. The digital ultrasonic interferometer for quality inspection of piezoelectric crystals. J. Eng. Appl. Sci., 11: 695-697.

Shrestha, P.K., 2010. Self-mixing diode laser interferometry. MSc Thesis, University of Waikato, New Zealand.

VanWiggeren, G.D. and R. Roy, 1999. Chaotic communication using time-delayed optical systems. Intl. J. Bifurcation Chaos, 9: 2129-2156.

Vidakis, A. and R. Santiago, 2015. Developing a laser-based biosensor with plasmonic accuracy. MSc Thesis, University of Catalonia, Spain.

Wei, L., 2011. Improving the performance of optical feedback self-mixing interferometry sensing. Ph.D Thesis, University of Wollongong, Australia.

Yeh, Y.L., 2008. Real-time measurement of glucose concentration and average refractive index using a laser interferometer. Opt. Lasers Eng., 46: 666-670.

Yu, Y., X. Qiang, Z. Wei and X. Sun, 1999. Differential displacement measurement system using laser self-mixing interference effect. Acta Opt. Sin., 19: 1269-1273.

Zhou, C. and C.H. Lai, 1999. Extracting messages masked by chaotic signals of time-delay systems. Phys. Rev. E., 60: 320-323.